High-Resolution, Large Field-of-View, and Multi-View Single Objective Light-Sheet Microscopy

Bin Yang[1*], Alfred Millett-Sikking[2], Merlin Lange[1], Ahmet Can Solak[1], Hirofumi Kobayashi[1], Andrew York[2], Loic A. Royer[1*]

[1]*Chan Zuckerberg Biohub, San Francisco, USA*
[2]*Calico Life Sciences LLC, South San Francisco, USA*

Light-sheet microscopy has become the preferred method for long-term imaging of large living samples because of its low photo-invasiveness and good optical sectioning capabilities. Unfortunately, refraction and scattering often pose obstacles to light-sheet propagation and limit imaging depth. This is typically addressed by imaging multiple complementary views to obtain high and uniform image quality throughout the sample. However, multi-view imaging often requires complex multi-objective configurations that complicate sample mounting, or sample rotation that decreases imaging speed. Recent developments in single-objective light-sheet microscopy have shown that it is possible to achieve high spatio-temporal resolution with a single objective for both illumination and detection. Here we describe a single-objective light-sheet microscope that achieves: (i) high-resolution and large field-of-view imaging via a custom remote focusing objective; (ii) simpler design and ergonomics by remote placement of coverslips; (iii) fast volumetric imaging by means of *light-sheet stabilised stage scanning* – a novel scanning modality that extends the imaging volume without compromising imaging speed nor quality; (iv) multi-view imaging by means of dual orthogonal light-sheet illumination. Finally, we demonstrate the speed, field of view and resolution of our novel instrument by imaging zebrafish tail development.

1 Introduction

In the past 15 years, light-sheet microscopy has become an essential imaging method for Biology[1,2]. It has pushed the limits of observability in Cell Biology[3], Developmental Biology[4–7], and Neuroscience[8,9]. The main reasons for this success are: its low photo-invasiveness[2,3,6], its high spatio-temporal resolution[3,10,11], and its ability to capture images of large and thick specimens such as embryos and organoids[4,12–14]. Light-sheet microscopy has been particularly impactful in Developmental Biology allowing the first *in-toto* volumetric reconstructions of embryonic development of model organisms such as Drosophila, Zebrafish, and Mouse[1,2,15]. The ability to image whole developmental arcs, and to follow hundreds of thousands of cells in space and time has shown the potential of light-sheet microscopy in answering long standing questions[15,16]. However, obstacles remain before light-sheet microscopy can completely fulfil its promises: state-of-the-art light-sheet microscopes are often not available commercially, require advanced skills to build, and force complex sample mounting strategies on users – all of which limit widespread adoption.

* Correspondence: loic.royer@czbiohub.org, bin.yang@czbiohub.org

Multi-view light-sheet microscopy. The main difficulty when imaging with light-sheet microscopy large living specimens such as zebrafish embryos, is the presence within the sample, of structures that absorb, refract and scatter, both the illumination and detection light. For example, in a zebrafish embryo, pigments will absorb light, the developing eyes will refract light, and in general, most biological tissue will cause light to scatter. These effects combine to degrade image quality impeding the acquisition of images of consistent quality over all sample regions. Multi-view imaging is an effective solution which consists in sectioning the sample with light-sheets from different complementary directions, and detecting from orthogonal directions. By illuminating and detecting from different orientations, obstacles to light propagation can be circumvented in some views versus others, and an image with better coverage and overall better quality can be computationally reconstructed[17]. While adaptive imaging approaches have been successfully demonstrated[11,18], they can't completely mitigate the need for multiple views. In practice, multi-view imaging is achieved by either surrounding the sample with 2 or more illumination and detection objectives[4,5,7], or by rotating the sample to change its relative position to the illumination and detection objectives[1]. From a specimen preparation perspective, this requires to carefully embed the sample within a transparent gel column[19]. This is at odds with the convenience of mounting samples on thin horizontal glass surfaces – something that biologists have been trained to do for the past hundred years, and that is compatible with standard slides, dishes, multiwell plates and microfluidics.

Improving sample mounting ergonomics. Inverted selective plane illumination microscopy[20,21] (iSPIM) and dual-view inverted selective plane illumination microscopy[22] (diSPIM) mitigate to some extent these sample mounting issues: these designs are compatible with standard inverted microscopy setups and thus allow for samples to be mounted on horizontal glass surfaces. Yet, at least two bulky objective lenses still need to be in close proximity to the sample – which is not sterile from sample to sample, and not compatible with multiwell plates or microfluidics. In addition, the large fluid volumes needed – due to the lens arrangement – can be costly and impractical for certain samples. In any case, the presence of multiple orthogonal objectives in close proximity to the sample results in an awkward interface between the biology and the optics – overall a major drawback. This ultimately limits adoption of multi-view light-sheet imaging[19], and of light-sheet technology in general for many users and applications.

Single objective light-sheet microscopy. The wide dissemination of multi-view light-sheet microscopy will require solv-

ing the ergonomics of sample mounting as well as simplifying the optical design. Recent developments have attempted to alleviate the necessity for orthogonal objectives. Initial attempts introduce small mirrors at the focal plane so that the excitation beam originating from the objective can be directed to the sample after reflection. Leica Microsystems devised a pair of small mirrors attached to the objective lens, converting a confocal microscope into a light-sheet microscope[23]. Galland *et al.* developed micro wells flanked by a $45°$ angled micro-mirror, achieving high numerical aperture (NA) imaging[24]. A more radical approach is to completely eliminate the need for additional objectives or mirrors and instead illuminate and detect from a single objective. The Oblique Plane Microscope (OPM) invention of 2008 restores the traditional coverslip boundary by passing light-sheet excitation and emission through a single primary objective[25], and then uses a tilted remote refocus in the downstream optics to image the equally tilted illumination plane. The remote refocus creates a virtual 3D copy of the object with minimal aberrations[26], which can then be re-imaged at a tilted or 'oblique' angle. An advantage of remote focusing is that it does not introduce additional aberrations[26]. OPM, as well as variations such as SCAPE[27,28], showed that light-sheet microscopy can be done with a standard microscope and sample interface, but seemingly exchanges this convenience for heavy losses in resolution and optical efficiency. The problem is that the tilted portion of the remote refocus loses a significant fraction of the emitted light, simply because the numerical aperture of the final objective is too low. An ideal objective would collect all of the emitted light, even with the additional tilt imposed by the oblique architecture, i.e. a full hemisphere of collection – a seemingly impossible requirement when objective half-angles are typically limited to $70°$.

Epi-illumination light-sheet microscope (eSPIM). Until recently, it was accepted that an OPM-style microscope necessarily meant compromising on the effective numerical aperture, and thus, on image resolution and signal. However, in 2018, Yang *et al.* showed that it is in fact possible to achieve uncompromised high spatio-temporal resolution with a single objective[29]. Using a water objective and coverslip assembly as the final objective, the numerical aperture could now equal the refractive index of air (1.0) i.e. the 'immersion medium' of the opposing objective in the remote refocus. This is the crucial insight: to make the elusive 'hemisphere' collection objective one simply needs a numerical aperture greater or equal than the index of the medium in which it operates. So, for example, an NA 1.0 water immersion objective has a modest $49°$ collection cone in water (a reasonable lens to manufacture), but in air this transforms to $90°$. So by imaging at the coverslip boundary, a water lens can indeed collect a solid angle of 2π from an air medium. There are however some additional considerations that complicate the eSPIM approach. The tertiary objective assembly is corrected for a water-coverslip-water medium and not water-coverslip-air. It can perform well if operated exactly at the surface of the coverslip, but deviations in alignment that push the image into the coverslip (or out into the air) will produce strong aberrations, so it can be challenging to keep aligned and hydrated. In addition, the bulkiness of the coverslip-water assembly requires longer working distance objectives in the remote refocus to avoid mechanical collision from the tilt. In practice this limits the choice of optics and tilt range, and can force a reduced numerical aperture on the air objective.

Pushing the limits with a bespoke objective design. Inspired by OPM and eSPIM, the AMS-AGY v1.0 objective[30] (aka Snouty) was developed to eliminate the previous trade-offs and compress the opto-mechanical difficulty into a single dedicated component (see Box 1 for details). The Snouty v1.0 objective enables 'bolt-on' single objective light-sheet designs with uncompromised numerical aperture which recently enabled sub-cellular imaging at sub-$200\,\mathrm{nm}$ resolution[31]. Yet, its design is constrained by mechanical and economic considerations, ultimately limiting the field of view to $150\,\mu\mathrm{m}$ diffraction-limited. Such a limited field cannot accommodate large living samples such as developing embryos and fundamentally limits imaging throughput. The usual solution to this problem is to tile the acquisition over multiple fields-of-view and computationally reconstruct an image of the whole specimen[32]. Unfortunately, tiled acquisitions trade imaging speed for field-of-view because the amount of information that can be acquired per second is – among other things – limited by the field of view. Therefore, what is really needed is a novel single-objective design that would be capable of multi-view imaging over a wide field-of-view, with uncompromised image resolution and speed.

High-resolution, large field-of-view, and multi-view single objective light-sheet microscopy. In this work, we demonstrate an instrument that achieves this goal by means of several innovations: First, we show how uncompromised image resolution and unprecedented field of view can be obtained by means of a novel custom tertiary objective. Second, we further improve sample mounting ergonomics by showing that it is possible to convert objectives between immersion and dipping states using remote focusing. Third, we introduce a new fast 3D scanning modality – *light-sheet stabilised scanning* (LS3) – that further extends the effective imaging volume without compromising imaging speed nor quality. Fourth, we show how to achieve multi-view imaging and enhance volumetric coverage and image quality with dual orthogonal illumination. Finally, we demonstrate these novel capabilities by imaging zebrafish tail development.

2 Results

We first describe the design and innovations of our instrument and characterise its resolution, field of view, and volumetric imaging capabilities. Finally, we demonstrate the high-speed, high resolution and large field-of-view of our single-objective dual light-sheet microscope by imaging zebrafish tail development for 2.2 hours – opening the door to many applications in developmental biology, and beyond.

BOX 1 Large field-of-view AMS-AGY v2.0 objective – aka *KingSnout*

The large field-of-view version 2.0 of the AMS-AGY NA 1.0 objective[30] features a monolithic glass tip with zero working distance; this tip is optically equivalent to an oil-coverslip-air interface but alignment-free and mechanically stable. The tip also features an anti-reflection coating to maximise collection from the full hemisphere of rays. The zero working distance is another critical feature; the large refractive index mismatch at the glass-air interface produces strong spherical aberrations that vanish only at this boundary. The high refractive index of the glass tip compresses the collection half-angle so the tip can be shaved off (Supp. Fig. 10) to allow a range of tilt angles from 0 to 55°. This excellent mechanical clearance allows image collection as close as 16 µm from a planar boundary. In practice this means the AMS-AGY objective can be paired with objectives with the highest numerical apertures and therefore the maximum collection efficiency. Infinity and color corrected, this component enables an extensive suite of design options. To overcome the limits on field of view of the first version, the AMS-AGY v2.0 objective has a three fold increased field-of-view (i.e. 450 µm diffraction limited and 450 µm to the shaved edge, see Supp. Fig. 10). The large field was partly achieved by increasing the budget for design and manufacture – it is a larger and more complex lens – but also by eliminating the margin between the diffraction limited field-of-view and the shaved edge. This enables the lens to be used 'off-axis' in the tightest of spaces without losing optical quality. AMS-AGY v2.0 is also ground at a more aggressive angle (55° vs 45°) which combined with the reduced margins gives the maximum clearance for tilting in the remote refocus. It is a strict upgrade to the v1.0 objective and compatible with all single objective light-sheet designs.
The specification of the AMS-AGY objectives are exactly as specified: NA 1.0 with fields of 150 µm (v1.0) and 450 µm (v2.0), where NA 1.0 actually means the lens will image at NA 1.0, not that it merely collects at this NA. How these specifications translate into the object space and the resulting volumetric imaging performance is subtle and beyond the scope of this work. However it should be noted that these objectives can be used beyond the specified fields, by up to a factor of approximately 1.7×, but not at NA 1.0. So a less genuine, but perhaps more typical specification would be NA 1.0 with fields of 250 µm (v1.0) and 750 µm (v2.0).

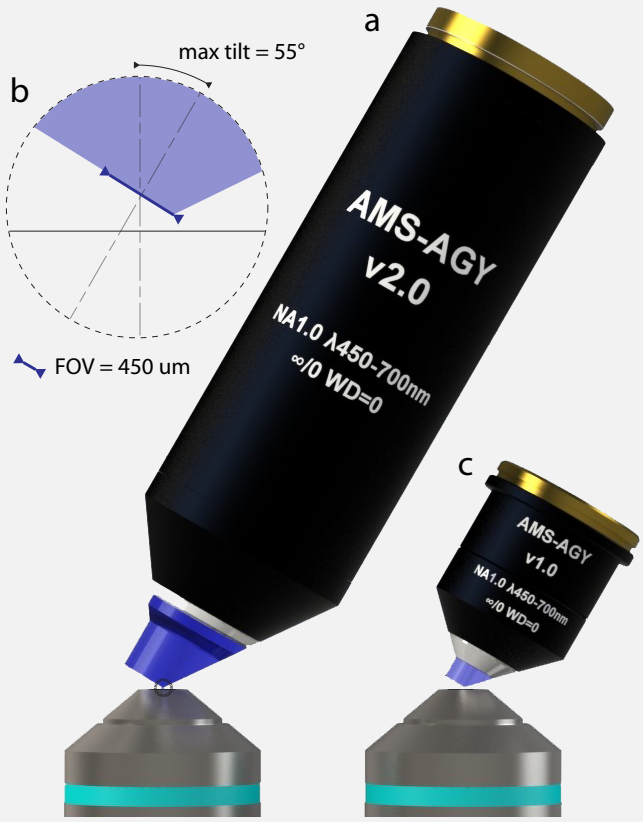

Instrument design and innovations.

Larger field-of-view by means of a custom objective. The first problem when attempting to image large samples such as a zebrafish embryos is the trade-off between resolution and field-of-view. This trade-off is particularly salient when illumination and detection light must pass through the same objective (as shown in Fig. 1a). In order to expand the field of view and retain the nominal high resolution at NA 1.0, we use a custom tertiary objective AMS-AGY v2.0 – the second instance of a family of objectives that are specifically designed for single-objective light-sheet microscopy (see Fig. 1b). These NA 1.0 objectives feature an air-glass imaging boundary and a zero working distance for maximum mechanical clearance and hemispherical collection in air. The objectives will image stigmattically at NA 1.0 over the specified fields (150um for v1.0 and 450um for v2.0) although they can be used well beyond these conservative specifications. Box 1 and Supplements gives technical details on the design and manufacture of this objective.

Remote coverslips. Another obstacle to the design of a single objective light-sheet microscope is the difficulty in finding suitable primary and secondary objectives compatible with the chosen sample mounting strategy: some objectives are immersion and others are dipping states. For example, in our instrument, we use a primary objective that does not require a coverslip (Olumpus XLUMPLFLN 20XW NA1.0, water) and a secondary objective that does require a coverslip (Olympus UPLXAPO20X). However, we also need a glass surface to hold the sample above the primary objective. This is the worst case scenario: the sample mounting requires that we have a coverslip where the optics forbid it, and the optics require we put a

coverslip in an inconvenient location: between the secondary and tertiary objectives. Instead of the optics dictating the sample mounting strategy, we want ideally to maximise flexibility and choice. How to solve this dilema? Fig. 1c illustrates our finding: remote focusing can be leveraged to move coverslips between object and remote spaces while maintaining optical equivalence. The coverslip needed by the secondary objective can be moved to support the sample – considerably simplifying the design. Importantly, we observe that image quality is the same, as shown in Supp. Fig. 5-6.

Light-sheet stabilised stage scanning. Volumetric scanning in a single objective light-sheet microscope can be done in three main ways: (i) by moving the imaging plane relative to the sample without moving the primary objective; (ii) by moving the primary objective relative to the sample but keeping the imaging plane fixed relative to the objective; (iii) by moving the sample relative to the primary objective and keeping the imaging plane fixed relative to the objective. The first approach is the fastest because, typically, it is implemented with a fast actuator such as a galvometer scanner. However, it has the most limited volumetric scanning range because the imaging plane cannot be moved arbitrarily far from the primary objective's optical axis. Moreover, large scans that move the light-sheet and detection planes away from the objective's axis can lead to aberrations and reduced image quality. The second, and third options, do not move the imaging plane relative to the objective and thus do not suffer from this effect. However, for the second option, a vertical (focus) scan of the detection objective is unpractical, because it is limited by the working distance of the lens. Finally, option three, often refereed to as stage scanning, is conventionally considered slow and cumbersome. Indeed, it must be done step-by-step to avoid motion blur – the stage stops moving during each camera exposure and resumes movement afterwards. This is slow because of the need to wait for high inertia mechanics to settle. Fast piezo stages are available, but have limited range and rapid step-by-step scanning leads to undesirable high-frequency sample shaking and vibrations. And yet, stage scanning advantages are enticing: effectively unlimited range and no need to displace optical parameters away from their optimum. If only stage scanning could be made fast without incurring motion blur nor sample shaking. Enter *light-sheet stabilised stage scanning* (LS^3), as shown in Fig. 1d and Supp. Fig.7, we move the stage continuously and use a counteracting motion of the light-sheet and detection planes – both actuated by a galvomneter scanner – to cancel out any relative motion between sample and imaging plane, but only during the exposure time of the camera. Since most cameras have a readout time of several milliseconds (e.g. $10ms$ for full frame imaging on a Flash 4.0 sCMOS) there is ample time for the imaging plane to be brought back quickly to the starting position before a new frame is acquired. All advantages of stage scanning are retained, while simultaneously benefiting from the advantages of high-speed galvometer-based scanning. The limits of this approach can be best understood by considering extreme cases: for example, *long* exposures and *fast* stage travel are possible but achieving stabilisation require a proportionally *long* travel of the imaging plane away from its optimal placement. In light of the typical exposures and travel speeds needed in practice, the only true limiting factors are camera speed and fluorophore brightness.

Dual orthogonal light-sheet illumination for multi-view imaging. As discussed earlier, large samples have occluding, refracting, and scattering structures that require multi-view imaging if one is to obtain good coverage and consistent image quality. We achieve dual-view imaging by flipping the light-sheet illumination and detection plane through $90°$ (see Suppl. Fig. 1B) to give a pair of complementary orthogonal views, as shown in Fig. 1e. In each view the emission path retains almost the full numerical aperture of the primary objective, but the orthogonal image planes benefit from the contrasting trajectories into the sample, in many cases avoiding obstacles and therefore returning complementary information that can be fused in post processing. The non-linear angular compression occurring between secondary and tertiary objectives also accounts for a lesser difference (see Supp. Fig. 4). Yet, to a large extent, both views share the same high-NA light collection optics.

Instrument characterisation.

Custom tertiary objective. The custom tertiary objective guarantees that most of the fluorescence light collected by the upstream optical train is imaged onto the camera. The nominal NA of the microscope is thus close to that of the primary objective O_1, i.e. 1.0. In practice, we note that the light is compressed towards one edge of the pupil of the tertiary objective O_3 along the x'-axis due to the air-glass interface between O_2 and O_3, as shown in Suppl. Fig. 3. As a result, the effective pupil function is no longer symmetric with respective to the optical axis along the x'-axis, as shown in Suppl. Fig. 4. Therefore, better resolution is achieved along the y-axis than along the x-axis.

Point-spread-function. We measured the point-spread-function (PSF) using $170\,\mathrm{nm}$ green fluorescence beads in both views. As described previously[29], the raw images are deskewed and rotated back to the coverslip-based coordinates for better comparison. The FWHMs are 541 nm, 430 nm and 1807 nm respectively along the $x-$, $y-$ and z-axes (see Fig. 2b and Suppl. Fig. 8). We note that the resolutions are not diffraction-limited and we do notice aberrations existing in the optical system, mostly originating from the primary objective. We also show that the same optical performance is maintained (see Suppl. Fig. 6) when we switch the coverslip from O_2 to O_1. This converts O_1 from a water dipping objective into a water immersion objective, and is important to achieve an inverted epi-fluorescence microscope. We also note that due to the asymmetry of the effective pupil function, the PSF is tilted with respect to the optical axis of O_3, i.e. the z'-axis. Our simulations suggest a tilt of $27°$ (see Suppl. Fig. D), but in

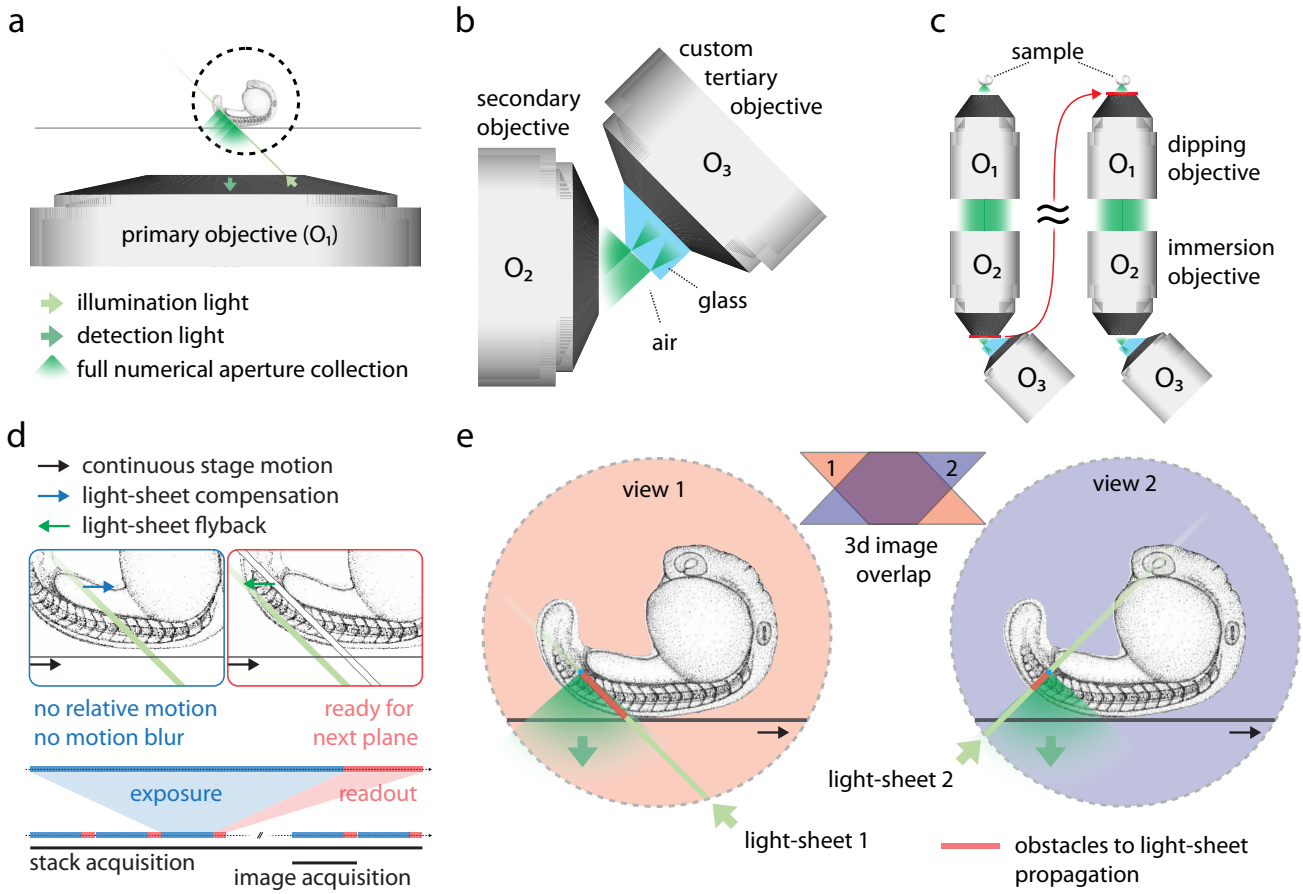

Figure 1: Design of a high-resolution, large field-of-view, and multi-view single objective light-sheet microscope. **(a)** In a single objective light-sheet microscope, the light-sheet excitation and emission pass through a single objective. In contrast to previous implementations, our instrument achieves high resolution imaging and does so over a wider field-of-view – sufficient to image large specimens such as zebrafish embryos. **(b)** Wide field oblique detection with uncompromised resolution is achieved by oblique remote focusing using a bespoke objective with a monolithic glass tip and zero working distance. The glass tip compresses the collection half-angle allowing a tilt range from 0 to 55° (see Box 1 for more details). **(c)** The choice of primary (O_1) and secondary (O_2) objectives is limited because some are dipping while others are immersion – considerably restricting the design space. However, we found that remote focusing lets you freely move coverslips between real and remote spaces. For example, assuming O_1 is dipping, and O_2 is immersion, the single coverslip for O_2 can be used to support the sample above O_1 instead of being inconveniently placed between O_2 and O_3. **(d)** Light-sheet stabilised scanning can turn the continuous motion of a long-range stage into a step-by-step relative motion between the sample and the imaged plane. This is practically equivalent to having a stage that is as fast as a galvometer scanner. This allows for motion-blur-less volumetric imaging over millimeters – only limited by camera speed and fluorophore brightness. Importantly, illumination and detection planes remain centered along the entire optical train to give optimal light collection, minimal aberrations, and thus pristine image quality. **(e)** In large specimens, light-sheet excitation is absorbed, refracted, scattered, and eventually loses all planar confinement. To improve coverage and image contrast, our instrument is capable of dual light-sheet excitation. For most points within the sample, one of the two light-sheet orientations will have a shorter penetration depth through the sample giving a more contrasted and complete image.

practice we noticed that the tilt is slightly higher, probably due to aberrations. As a result, the two views PSFs' are not exactly orthogonal to each other – unlike for diSPIM[22] configurations. They most likely provide limited complementary information, something that could be exploited using multi-view deconvolution[17].

Field-of-view. Fig. 2a shows the imaging volume of our microscope. The PSF is consistent across $550\,\mu\mathrm{m}$ along the y-axis and $250\,\mu\mathrm{m}$ along the z-axis. The scanning range using the galvometer scanner is limited to about $300\,\mu\mathrm{m}$, due to clipping of the laser beam by the tube lenses. Using our light-sheet stabilised stage scanning, we achieve much larger scanning range with no compromise of imaging quality nor speed. We do note that when imaging smaller samples, galvometer scanning is faster because the galvometer flyback time is just a few milliseconds, whereas it lasts hundreds of milliseconds for the stage. Our instrument is capable of both scanning modes, providing flexibility depending on the desired volume dimensions. The imaging speed largely depends on the scanning range, but also on signal level, scanning step size, etc. For an imaging volume of $1000\,\mu\mathrm{m} \times 550\,\mu\mathrm{m} \times 250\,\mu\mathrm{m}$, we typically achieve an imaging speed of about 10 to 30 seconds per volume. By tuning imaging parameters according to experimental requirements, much higher speed are achievable similarly to other single objective light sheet implementations[28,29].

Imaging zebrafish tail development. To demonstrate our microscope's field of view, resolution and speed, we imaged zebrafish tail development 24 hours post fertilisation for 2.2 hours. Fig. 3a shows that nearly the whole tail can be imaged from the posterior part of the tail (the tail bud) to the anterior trunk, spanning a little more than a millimeter of tissue along the posterior-anterior axis. Stabilised light-sheet scanning is key to acquire such large and high-quality volumes. The two views obtained by dual orthogonal illumination are acquired to maximise coverage and image quality. Indeed, as shown in Fig. 3bc these views are complementary in terms of contrast and coverage. Depending on the region inspected, one view, or the other, will be better. In general, we find a good agreement between our observations (see Fig. 3c) and our assumption that given a point within the sample, the longer the light-sheet penetration depth, the lesser the image quality for the corresponding view. For each time point we obtain a single fused image (see Fig. 3d) consisting of $4000 \times 2000 \times 360$ voxels. Both views are acquired every 40 seconds making it possible to closely follow cell division (see Fig. 3ef). This is important because many applications in developmental biology require to track cells and follow lineages – something that is very difficult or nearly impossible if cells divide faster than ones ability to image them.

3 Conclusion

We have shown that our novel single objective light sheet microscope can achieve high spatio-temporal resolution over a large field-of-view. We achieve a resolution of approximately $400nm$ to $500nm$ lateraly and $1.8um$ axially with a effective imaging volume of $550um \times 250um$ by a few millimeters (last dimension is unconstrained). Importantly, our instrument achieves that performance without forcing unconventional sample mounting procedures on the user – especially when compared with standard multi-view lightsheet microscopes[5,11]. Developmental biologists can now mount samples in a convenient manner, image multiple specimens in parallel[33], flow drugs and other chemicals with microfluidics, and leveraging the free space above the sample to combine imaging with other sensing or manipulation schemes such as e.g. patch clamping and mechanical perturbation.

4 Methods

Optical setup. Supp. Fig. 1 shows the detailed optical setup. A primary objective (O_1, Olumpus XLUMPLFLN 20XW NA1.0, water) is used to both generate an oblique light-sheet in the sample and to collect the fluorescence. A series of tube lenses (TL_1 to TL_6) conjugate the pupils of O_1 and O_2 so that an intermediate image of the sample at O_1 was formed at the secondary objective O_2 (Olympus UPLXAPO20X). The intermediate image has a uniform magnification of 1.33, equal to the refractive index ratio of the medium of O_1 versus that of O_2, making the optical train aberration-free over a reasonable volume. [34]. A custom tertiary objective O_3 (AMS-AGY v2.0, see box 1) is oriented by $45°$ with respect to O_2. The fluorescence is filtered by either individual bandpass filters (Chroma ET525/50, ET605/70) or a quad-band filter (Chroma ZET405/488/561/640) and then detected by a scientific complementary metal-oxide semiconductor (sCMOS) camera (Hamamatsu ORCAFlash 4.0). The pixel size of the cameras at the sample space is $219nm$ (TL_7 - Thorlabs is-A) for PSF calibration and $265nm$ (TL_6 - Thorlabs TTL165-A) for imaging to be able to capture the desired field of view. Objective O_3 was mounted on a piezo stage (PI Fast PIFOC Z-Drive PD72Z1SAQ) so that its focus can be finely tuned.

Remote coverslip. The coverslip required for the secondary objective is removed and placed instead between the sample and the primary objective. This has a negligible effect on optical performance but enables the imaging of samples prepared on coverslips in an epi-fluorescence mode.

Light-sheet incident angle adjustment. A 2-axes galvo mirrors (Cambridge $10mm$ 6SD12056) are conjugated with the sample plane so that rotating the two mirrors resulted a rotation of the excitation beam at the sample plane. In particular, the incident angle of the light-sheet at the focal space of O_1 can be adjusted by one of the mirrors to $45°$ with respect to the optical axis. The effective excitation NA is estimated to be 0.08 at this incident angle.

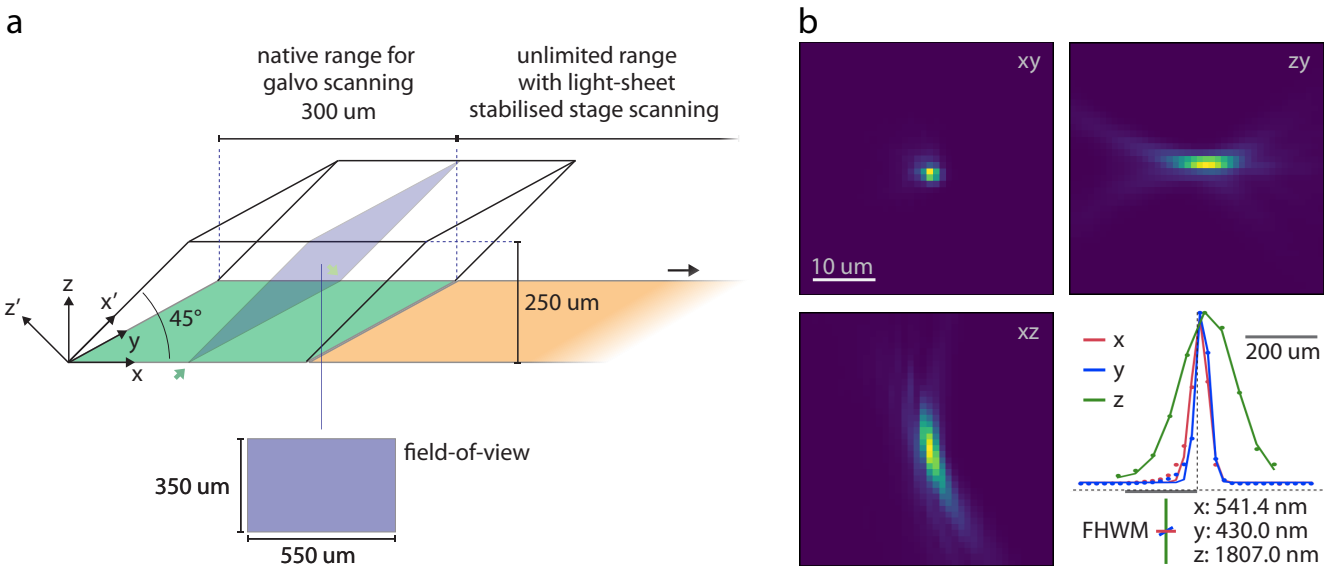

Figure 2: Imaging volume and point spread function of the microscope. **(a)** Imaging volume geometry. The optical axis of the microscope is along the z-axis. The coverslip is parallel to the xy plane. The sample is illuminated by an oblique light sheet, in the $x'y$ plane. The scanning is along the x direction. **(b)** Point spread function obtained by imaging $170\,\mathrm{nm}$ green fluorescence beads. Projections along xy, xz, and zy, centered line profiles along x, y, and z, as well as full-half-witdh-maximum (FHWM) measurements.

Multi-view switching. Two switching galvo mirrors are used to create two views of the object at the sample space. By adjusting the angles of the two galvo mirrors, the light is reflected either by two reflective mirrors or only one. The operating principle is similar to that of a Dove prism. Moreover, the switching module also changes the incident angle of the light-sheet between $+45°$ and $-45°$ since the excitation light also passes through this module.

Illumination and detection scanning. Another Galvo mirror (Cambridge Tech, 20mm galvo, 6SD12205) is conjugated to the pupil planes of both O_1 and O_2. Rotating the galvometer actuated mirror scans the oblique light-sheet across the sample (along the x axis), with the incident angle kept at $45°$. The Galvo mirror also descans the intermediate image at the focal space of O_2 so that the intermediate image is always projected at the focal plane of O_3. Using the galvometer for 3D scanning allows for faster imaging compared to stage scanning – but at the cost of a limited scan range of approximately $300um$.

Motorised sample stage. A motorised stage (ASI MS-2000) is used to position the sample and to perform scanning for volumetric imaging. During acquisition of each frame, stage scanning is combined with galvo descanning to stabilise the imaging plane (coplanar light-sheet and detection planes) relative to the sample. In the absence of relative motion between the sample, light-sheet and detection plane, no motion blur occurs. Stabilised light-sheet stage scanning allows for much longer ranges compared to galvometer-based scanning. It is only limited by the range of travel of the stage, in our case $100mm$. Importantly, illumination and detection planes remain fixed and optimally placed at the center of O_1 and O_2 native axes thus guaranteeing optimal light collection, minimal aberrations, and thus optimal image quality.

Microscope control software. The microscope is primarily controlled by the open-source, freely available software *Micro-Manager 2.0 Gamma*[35]. A custom-developed micro-manager script sets up the acquisition order and stores the hyperstack data in TIFF files. A NI compact DAQ system (cDAQ-9178, NI 9263 4-Channel AO module, NI 9401 8-Channel DIO module) was controlled by custom Python code (using the NI-DAQmx python API) to synchronise the devices, including camera, motorized stage, galvo mirrors and lasers during data acquisition. A *triggerscope* (Advanced Research Consulting, TriggerScope 3B) provides additional analog output channels to control the 2-axes galvos that are responsible for light sheet incident angle adjustment. A water immersion micro-dispenser is controlled by custom Python code to supply water to the primary objective during long term recordings.

Data processing. Pycro-manager[36] is used to readout the multi-dimensional data saved by Micro-Manager. Each 3D stack is first deskewed and then rotated to coverslip-based coordinates[3] using pycudadecon (link: https://github.com/tlambert03/pycudadecon). The 3D stacks from the two views are then registered based on cross-correlation, and combined with discrete cosine transform based fusion[37]. The multi-dimensional dataset is visualized using napari[38].

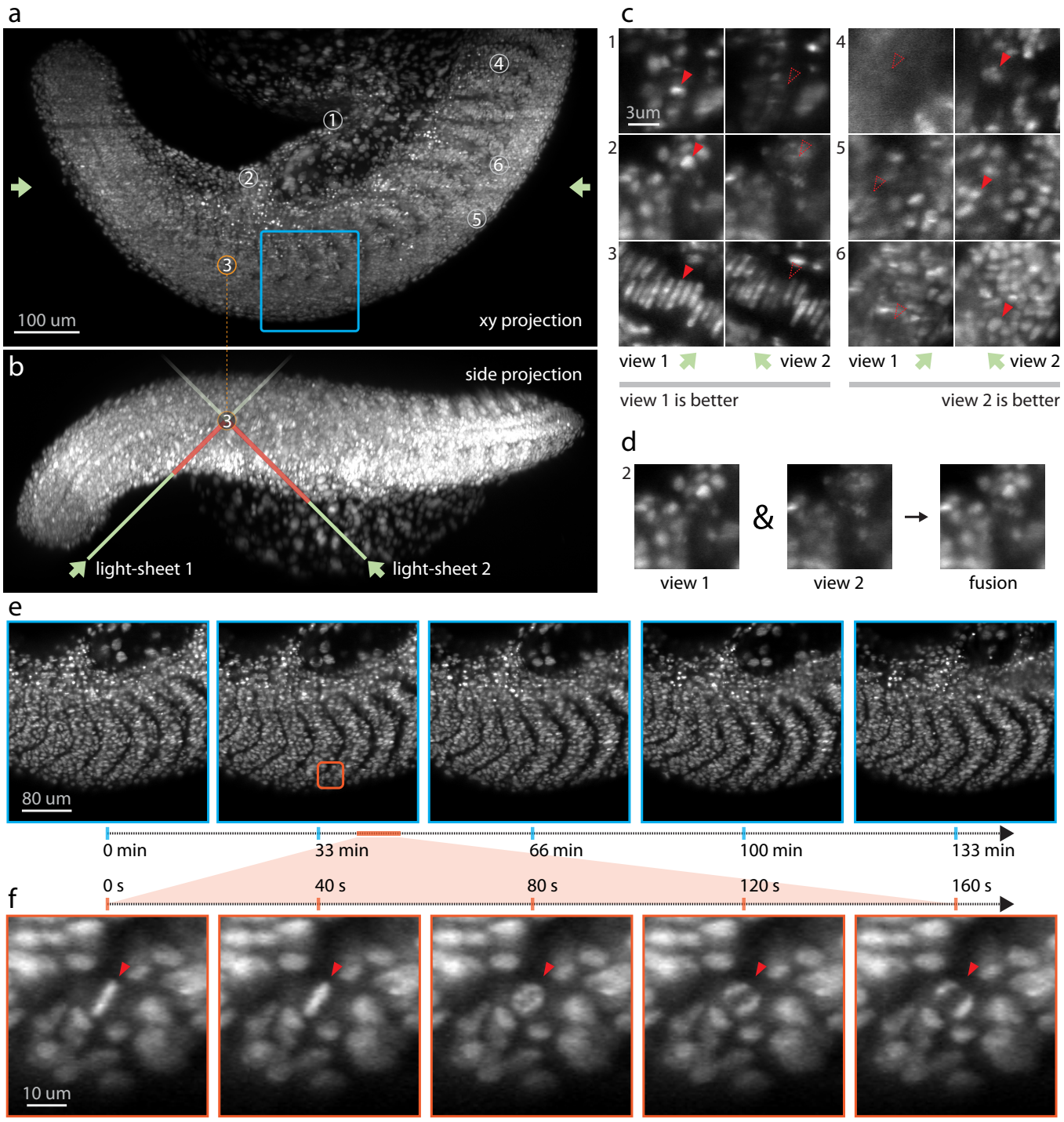

Figure 3: Imaging zebrafish development. **(a)** Axial max projection showing the whole zebrafish tail at 24 hours post fertilisation with histones labelled with mCherry. Imaging volume is $1064\,\mu m \times 532\,\mu m \times 287\,\mu m$ consisting in $4000 \times 2000 \times 360$ voxels per view for a total of 5.7 billion voxels acquired every 40 seconds. **(b)** Side projection illustrating how the two light-sheets enter the sample at $45°$ to reach a given point within the sample. Depending on the sample geometry and placement, one of the two light-sheets will have a shorter path to reach that point and will have less chances to be absorbed, refracted or scattered. Consequently, the corresponding view's image will be more complete and better contrasted. **(c)** Example regions that demonstrate the complementarity of the two views. In some regions (left) the first view has better image quality, whereas in other regions (right) it is the second view that has better image quality. **(d)** After registration, the two views can be fused together to obtain one image that is strictly better. **(e)** Timelapse max-projection frames over a 2.2 hour period centered on the dorsomedial tail. We see the accentuation of the boundary between neighbouring somites. **(e)** Spatio-temporal zoom centered around a cell division, single plane slice. Despite the large field of view both views are acquired every 40 seconds making it possible to follow the intermediate steps during mitosis – an important capability for achieving, for example, accurate lineage tracking.

Sample preparation. Zebrafish husbandry and experiments were conducted according to protocols approved by the UCSF Institutional Animal Care Use Committee. First, zebrafish were dechorionated with a pair of sharp forceps underneath a binocular dissecting microscope, and incubated at least 5 minutes in a solution of fish water and tricaine (0.016%). Embryos were gently pipetted into a 1% solution of low gelling point agarose (Sigma, A0701) cooled at $37°C$. The embryos, together with approx. $1ml$ of 1% agarose, were placed in a glass-bottomed petri dish (Stellar Scientific Cat. No 801001). Using some capillary needle, the embryo is gently positioned at the center of the dish and positioned in the desired orientation, here laterally. When the agarose is solidified, the dish is flooded with embryo medium and 0.016% tricaine.

Bibliography

1. Huisken, J., Swoger, J., Del Bene, F., Wittbrodt, J. & Stelzer, E. H. Optical sectioning deep inside live embryos by selective plane illumination microscopy. *Science* **305**, 1007–1009 (2004).

2. Keller, P. J., Schmidt, A. D., Wittbrodt, J. & Stelzer, E. H. K. Reconstruction of Zebrafish Early Embryonic Development by Scanned Light Sheet Microscopy. *Science* **322**, 1065–1069 (2008).

3. Chen, B.-C. *et al.* Lattice light-sheet microscopy: imaging molecules to embryos at high spatiotemporal resolution. *Science* **346** (2014).

4. Tomer, R., Khairy, K., Amat, F. & Keller, P. J. Quantitative high-speed imaging of entire developing embryos with simultaneous multiview light-sheet microscopy. *Nat. Methods* **9**, 755 (2012).

5. Krzic, U., Gunther, S., Saunders, T. E., Streichan, S. J. & Hufnagel, L. Multiview light-sheet microscope for rapid in toto imaging. *Nature methods* **9**, 730–733 (2012).

6. Huisken, J. & Stainier, D. Y. Selective plane illumination microscopy techniques in developmental biology. *Development* **136**, 1963–1975 (2009).

7. Chhetri, R. K. *et al.* Whole-animal functional and developmental imaging with isotropic spatial resolution. *Nature methods* **12**, 1171–1178 (2015).

8. Lemon, W. C. *et al.* Whole-central nervous system functional imaging in larval drosophila. *Nature communications* **6**, 1–16 (2015).

9. Ahrens, M. B., Orger, M. B., Robson, D. N., Li, J. M. & Keller, P. J. Whole-brain functional imaging at cellular resolution using light-sheet microscopy. *Nature methods* **10**, 413–420 (2013).

10. Chakraborty, T. *et al.* Converting lateral scanning into axial focusing to speed up three-dimensional microscopy. *Light: Science & Applications* **9**, 165 (2020).

11. Royer, L. A. *et al.* Adaptive light-sheet microscopy for long-term, high-resolution imaging in living organisms. *Nat. Biotechnol.* **34**, 1267–1278 (2016).

12. Voigt, F. F. *et al.* The mesospim initiative: open-source light-sheet microscopes for imaging cleared tissue. *Nature methods* **16**, 1105–1108 (2019).

13. Dekkers, J. F. *et al.* High-resolution 3d imaging of fixed and cleared organoids. *Nature protocols* **14**, 1756 (2019).

14. Glaser, A. K. *et al.* 837-Light-sheet microscopy for slide-free non-destructive pathology of large clinical specimens. *Nature Biomedical Engineering* **1**, s41551–017–0084–017 (2017).

15. McDole, K. *et al.* In toto imaging and reconstruction of post-implantation mouse development at the single-cell level. *Cell* **175**, 859–876 (2018).

16. Shah, G. *et al.* Multi-scale imaging and analysis identify pan-embryo cell dynamics of germlayer formation in zebrafish. *Nature communications* **10**, 1–12 (2019).

17. Preibisch, S. *et al.* Efficient bayesian-based multiview deconvolution. *Nature methods* **11**, 645–648 (2014).

18. Liu, T.-L. *et al.* Observing the cell in its native state: Imaging subcellular dynamics in multicellular organisms. *Science (New York, N.Y.)* **360** (2018).

19. Kaufmann, A., Mickoleit, M., Weber, M. & Huisken, J. Multilayer mounting enables long-term imaging of zebrafish development in a light sheet microscope. *Development* **139**, 3242–3247 (2012).

20. Wu, Y. *et al.* Inverted selective plane illumination microscopy (ispim) enables coupled cell identity lineaging and neurodevelopmental imaging in caenorhabditis elegans. *Proceedings of the National Academy of Sciences* **108**, 17708–17713 (2011).

21. Capoulade, J., Wachsmuth, M., Hufnagel, L. & Knop, M. Quantitative fluorescence imaging of protein diffusion and interaction in living cells. *Nature biotechnology* **29**, 835–839 (2011).

22. Wu, Y. *et al.* Spatially isotropic four-dimensional imaging with dual-view plane illumination microscopy. *Nature biotechnology* **31**, 1032–1038 (2013).

23. Knebel, W. & Sieckmann, F. Method and device for illuminating a sample (2011).

24. Galland, R. *et al.* 3d high-and super-resolution imaging using single-objective spim. *Nature methods* **12**, 641–644 (2015).

25. Dunsby, C. Optically sectioned imaging by oblique plane microscopy. *Opt. Express* **16**, 20306–20316 (2008).

26. Botcherby, E. J. *et al.* Aberration-free three-dimensional multiphoton imaging of neuronal activity at khz rates. *Proceedings of the National Academy of Sciences* **109**, 2919–2924 (2012).

27. Bouchard, M. B. *et al.* Swept confocally-aligned planar excitation (scape) microscopy for high-speed volumetric imaging of behaving organisms. *Nature photonics* **9**, 113–119 (2015).

28. Voleti, V. *et al.* Real-time volumetric microscopy of in vivo dynamics and large-scale samples with scape 2.0. *Nature methods* **16**, 1054–1062 (2019).

29. Yang, B. *et al.* Epi-illumination spim for volumetric imaging with high spatial-temporal resolution. *Nature methods* **16**, 501–504 (2019).

30. Millett-Sikking, A. & York, A. G. High NA single-objective lightsheet. *Github.io* (2019).

31. Sapoznik, E. *et al.* A single-objective light-sheet microscope with 200 nm-scale resolution. *bioRxiv* (2020).

32. Hörl, D. *et al.* Bigstitcher: reconstructing high-resolution image datasets of cleared and expanded samples. *Nature Methods* **16**, 870–874 (2019).

33. Daetwyler, S., Günther, U., Modes, C. D., Harrington, K. & Huisken, J. Multi-sample SPIM image acquisition, processing and analysis of vascular growth in zebrafish. *Development* **146** (2019).

34. Botcherby, E. J., Juskaitis, R., Booth, M. J. & Wilson, T. Aberration-free optical refocusing in high numerical aperture microscopy. *Optics Letters* **32**, 2007–2009 (2007).

35. Edelstein, A. D. *et al.* Advanced methods of microscope control using μmanager software. *Journal of biological methods* **1** (2014).

36. Pinkard, H., Stuurman, N. & Waller, L. Pycro-manager: open-source software for integrated microscopy hardware control and image processing. *arXiv:2006.11330 [q-bio]* (2020).

37. Cao, L. *et al.* Multi-Focus Image Fusion Based on Spatial Frequency in Discrete Cosine Transform Domain. *IEEE Signal Processing Letters* **22**, 220–224 (2015). Conference Name: IEEE Signal Processing Letters.

38. Sofroniew, N. *et al.* napari/napari: 0.3.7rc3 (2020).

Supplementary Information All supplementary information, code, blueprints and tutorials can be found at: *github.com/royerlab/hr-lf-mv-SOLS*

Acknowledgements We would like to thank the Bioengineering team at CZ Biohub for loaning us the water immersion micro dispenser. We thank Nico Sturrman from UCSF for his help on Micro-Manager and Jan Huisken (Morgridge Institute for Research) for sharing the Tg(h2afva:h2afva-mch). Funding for this work was provided by the Chan Zuckerberg Biohub. We thank Calico Life Sciences LLC for funding the development of the AMS-AGY V2.0 objective and for granting a loaned objective.

Correspondence Correspondence and requests for materials should be addressed to Loic A. Royer (email: loic.royer@czbiohub.org, twitter: @loicaroyer) and Bin Yang (email: bin.yang@czbiohub.org, twitter: @Bin_YANG_Optics).